Numerical simulation study on the offshore oscillating water column OWC integrated into a floating breakwater using CFD

Madjid Ghodsi Hassanabad, Mojtaba Shegeft

Abstract—**In this paper, hydrodynamic performance on oscillating water column (OWC) as a wave energy converter and a floating breakwater are studied via a 3D and 2D computational fluid dynamics (CFD) modelling. In order to make OWC device more Cost-effective in production and use, compared to other form of wave energy converters, using OWC devices with other offshore or coastal structures such as breakwaters is suggested. In This way, the wave energy can be attenuated to maintain costal structures in harbour zones, and in the same time energy can be gained from the ocean so the costs of producing OWC devices will be reduced through a integrate solution. In this research, the numerical results of 3D model of OWC chamber with parabolic side walls and flat side walls are investigated then 2D numerical model are studied to analyze the performance of OWC as a floating breakwater to do that different types of OWC models analyzed. In the model, Finite volume method has been used and the continuity and momentum equations were selected as the governing equations. Shear Stress Transport (SST) k-omega turbulence model is implemented to the Reynolds Stresses in RANS equations due to the high amount of turbulence in this system. Also, interaction between water and air is analyzed with the Volume of Fraction (VOF) method. Finally, according to the numerical models the best model is selected due to the damping of the waves and its performance.**

Keywords—*CFD,* **floating breakwater, Oscillating water column (OWC), wave attenuation,**

I. Introduction

RENEWABLE energy is an urgent matter in the world. Due to the reduction of fossil fuels and many irreversible harms they may cause, investigation in this industry and finding alternative sources of energy can be convenient. Wave energy could be a good fit. In order for this sources of energy to be useful, it needs to be captured and transformed into useful energy such as electricity. Among the different techniques used for wave energy converters, the Oscillating Water Column (OWC) devices stand as one of the most promising ones. In addition, its inherent simplicity is presumably the greatest advantage of OWC as a wave energy convector device which can generate sustainable energy, therefore using OWC devices can be convincing in many countries.

In order to make OWC device more Cost-effective in production and use, compared to other form of wave energy converters, using OWC devices with other offshore or coastal structures such as breakwaters is suggested. In This way, the wave energy can be attenuated to maintain costal structures in harbour zones, and in the same time energy can be gained from the ocean so the costs of producing OWC devices will be reduced through integrate solutions, simple manufacture and ease of installation to facilitate a competitive cost of energy in commercial.

The Structure of OWC devices consists of a large chamber, one end is open to the sea, and the other leads in to a orifice, when a wave approaches the device water is forced into the chamber, applying pressure on the air, already trapped inside the structure. As a result of this huge pressure the air escapes to atmosphere through the turbine on the other side of orifice, thereby producing electricity. When the wave retreats and the water surface level falls, the air from the outside the orifice is sucked back in to the chamber. As the water surface level inside the chamber moves up and down, it compresses and decompresses the air, respectively.as a result, electricity continues to be generated.

One of the goals of the present project is to promote the use of this device by increase the hydrodynamic performance of OWC devices integrated into a breakwater. So further investigation such as numerical (CFD) modelling need to be done to consider all challenges such as convert wave energy into a useful energy form, adaptability to a wide variety of different locations and ocean condition, survivability in the ocean over time and in storm condition. Due to the lack of fully understanding the OWC device, further studies are needed. According to the specific area.

Evance [1] studied OWC analytical model as a pair of parallel vertical plates, based on linear water wave theory. Then the wave power absorption by systems of oscillating surface pressure distributions was developed by Evance [2]. Many researchers have focused on

Paper ID number: 1747. Conference track: Wave hydrodynamic modelling.

M. G. Hassanabad is with Department of Marine Science and Technology, Tehran Science and Research Branch, Islamic Azad University, Tehran, Iran. (m.ghodsi@srbiau.ac.ir).

M. Shegeft is with Department of Marine Science and Technology, Tehran Science and Research Branch, Islamic Azad University, Tehran, Iran. (Mojtaba.shegeft@gmail.com).

hydrodynamic analysis of OWC power plant (eg, Thiruvenkatasamy et al. [3], Josset and Clement [4], João C Henriques et al. [5]). McKinley et al. [6] studied the development of a Pseudo-3D testing technique for the prediction of extreme loads on an oscillating wave surge converter. Their investigations show that the hydrodynamics and magnitudes of slams experienced by device in a 2D environment vary significantly from those experienced in the more realistic 3D environment. Elhanafi [7] investigated the prediction of regular wave load on a fixed offshore OWC using CFD. Then, he continued his studies on Experimental and numerical model [8]. Due to the lack of fully understanding the OWC device, further studies are needed either experimentally, numerically, or a combination of these methods.

II. MATHEMATICAL FORMULAE

It is assumed that the fluid is incompressible. The VOF model can model two or more immiscible fluids by solving a single set of momentum equations and tracking the volume fraction of each of the fluids throughout the domain for the q^{th} phase, this equation has the following form:

$$\frac{1}{\rho_q}\left[\frac{\partial}{\partial_t}(a_q\rho_q) + \nabla.(a_q\rho_q\overrightarrow{v_q}) = S_{a_q} + \sum_{p=1}^{n}(\dot{m}_{pq} - \dot{m}_{qp})\right] \quad (1)$$

$$\sum_{q=1}^{n} a_q = 1 \quad (2)$$

Where $\dot{m}_{qp}$the mass transfer from phase q to phase p , $\dot{m}_{pq}$is the mass transfer from phase p to phase q. The source term S_{a_q} is zero.

In the single fluid model, the phase function a_q is equal to 1 in water and 0 in air. The interface is defined by a_q=0.5. The magnitude of the physical characteristics of the fluids depends on the local phase. They are defined as:

$$\rho = \rho_1 \text{ And } \mu = \mu_1 \text{ if } a_q \geq 0.5$$
$$\rho = \rho_0 \text{ And } \mu = \mu_0 \text{ if } a_q < 0.5 \quad (3)$$

Where ρ_0,ρ_1, μ_0 and μ_1 are the densities and viscosities of fluid 0 and 1, respectively [9].

The mixture of air and water is considered as a fluid of variable density. The dynamic viscosity coefficient of the fluid are defined as:

$$\rho = \alpha_0\rho_0 + \alpha_1\rho_1 \quad (4)$$

$$\mu = \alpha_0\mu_0 + \alpha_1\mu_1 \quad (5)$$

Where α_0 and α_1 are voulume fraction of air and water respectively.

The advanced turbulence model is based on Reynolds averages of the governing equations. In Reynolds averaging, the solution variables in the instantaneous Navier-Stokes equations are decomposed into the mean and fluctuating components. Substituting expressions of this form for the flow variables into the instantaneous continuity and momentum equations and taking a time (or ensemble) average yields the ensemble-averaged momentum equations. They can be written in Cartesian tensor form as:

$$\frac{\partial\rho}{\partial t} + \frac{\partial}{\partial x_i}(\rho u_i) = 0 \quad (6)$$

$$\frac{\partial}{\partial t}(\rho u_i) + \frac{\partial}{\partial x_j}(\rho u_i u_j) = -\frac{\partial p}{\partial x_i} + \frac{\partial}{\partial x_j}\left[\mu\left(\frac{\partial u_i}{\partial x_j} + \frac{\partial u_j}{\partial x_i} - \frac{2}{3}\delta_{ij}\frac{\partial u_l}{\partial x_l}\right)\right] + \frac{\partial}{\partial x_j}(-\rho\overline{u_i'u_j'}) \quad (7)$$

The equations (5) and (6) are called ''Reynolds-averaged'' Navier-Stokes (RANS) equations. According to equation (6) ''Reynolds stresses'' $(-\rho\overline{u_i'u_j'})$ represents the effects of turbulence.

Features of the Shear-Stress Transport (SST) K omega model were more accurate and reliable for this numerical model.

$$\frac{\partial}{\partial_t}(\rho k) + \frac{\partial}{\partial x_i}(\rho k u_i) = \frac{\partial}{\partial x_j}\left(\Gamma_k\frac{\partial k}{\partial x_j}\right) + G_k - Y_k + S_k \quad (8)$$

$$\frac{\partial}{\partial_t}(\rho\omega) + \frac{\partial}{\partial x_j}(\rho\omega u_i) = \frac{\partial}{\partial x_j}\left(\Gamma_\omega\frac{\partial\omega}{\partial x_j}\right) + G_\omega - Y_\omega + D_\omega + S_\omega \quad (9)$$

Where the term G_k represents the production of turbulence kinetic energy. G_ω represents the generation of ω. Γ_k and Γ_ω indicate the effective diffusity of k and ω, respectively. Y_k and Y_ω indicate the dissipation of k and ω due to turbulence. D_ω represents the cross-diffusion term. S_k and S_ω are user-defined source terms [10,11]

The equation was solved for hydrodynamic analysis is potential equation. The boundary conditions were solid wall B.C., kinematic and dynamic free surface B.C., far field B.C. (Sommerfeld), and symmetry B.C. [12, 13]. BEM was selected as a numerical method for its simplicity in mesh generation and rapid processing in PDE solving. It assumed that boundary conditions are nonlinear and finite difference method was used for discretization of boundary conditions. Also, solving domain divided into 3 zones for preventing singularities (zoning method).

Another part of the problem is the modelling of the air volume enclosed in the OWC chamber above the inner free surface. The air pressure P(t) in the chamber is a new variable for which a new equation is necessary. This pressure reacts on the hydrodynamic problem through the dynamical free-surface condition. Hydrodynamics and aerodynamics are therefore strongly coupled. Fig. 1 shows a schematic view of OWC chamber with trapped air parameters on it.

The final form of pressure equation is as follows:

$$\frac{\dot{P}_k(t)}{P_k(t)+P_0}=\gamma\left[-\frac{P_k(t)}{K_t V(t)}\left(1-\varepsilon\frac{(P_k(t)+P_0)^{1/\gamma}-P_0^{1/\gamma}}{(P_k(t)+P_0)^{1/\gamma}}\right)+\frac{Q_w^k(t)}{V^{k-1}(t)-\Delta t\,Q_w^k(t)}\right] \quad (10)$$

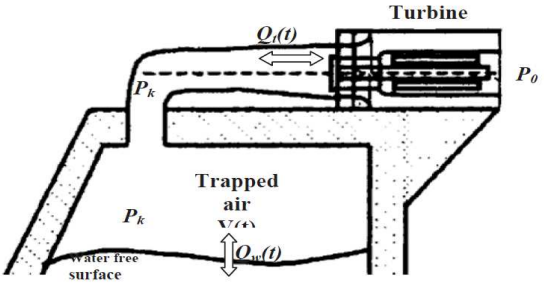

Fig. 1. Scheme of OWC chamber.

The dimensionless and discrete shape of this equation is as follows.

$$\hat{P}_k^k(t)=\hat{P}_k^{k-1}(t)+\gamma\Delta\hat{t}(\hat{P}_k^{k-1}(t)+\hat{P}_0)$$
$$\left[-\frac{\hat{P}_k^{k-1}(t)}{\hat{K}_t(\hat{V}^{k-1}(t)-\Delta\hat{t}\,\hat{Q}_w^k(t))}\left(1-\varepsilon\frac{(\hat{P}_k^{k-1}(t)+P_0)^{1/\gamma}-P_0^{1/\gamma}}{(\hat{P}_k^{k-1}(t)+P_0)^{1/\gamma}}\right)+\frac{Q_w^k(t)}{V^{k-1}(t)-\Delta t\,Q_w^k(t)}\right] \quad (11)$$

In this regard, new dimensionless parameters are introduced which are defined as follows.

$$\hat{P}=\frac{P}{\rho g L}\ ;\ \hat{Q}=\frac{Q}{L^2\sqrt{Lg}}\ ;\ \hat{V}=\frac{V}{L^3}\ ;\ \hat{K}_t=\frac{K_t}{\rho}\sqrt{\frac{L^3}{g}} \quad (12)$$

In which ρ is the density of the sea water.

III. 3D NUMERICAL MODEL OF OWC

In the first step, 2 types of OWC models were compered numerically, Three-dimensional OWC with flat side walls and numerical model of OWC chamber with parabolic side walls. In the 3D modes, some measures are taken to ensure that the power absorbed is as much as possible. In this section, two hypothetical OWC offshore power plants with two different geometries are analysed and compared.

A. 3D OWC with flat side walls

In this research, it is assumed that the wave's direction are perpendicular to the coast and move towards the OWC.

In order to achieve the efficiency of the OWC, it is necessary to calculate the power output of the power plant. In the present problem, the output power is considered to be equivalent to the air power transmitted

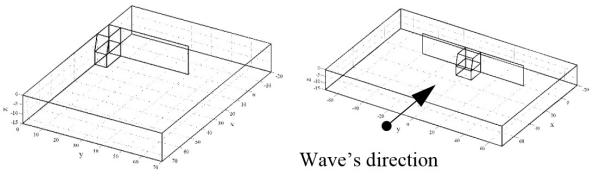

Fig. 2. Geometry of the OWC with flat side walls.

from the turbine.

$$Power\ =\left|Q_t(t)\times P_k(t)\right|=\frac{P_k^2(t)}{K_t}=\frac{(P(t)-P_0)^2}{K_t} \quad (13)$$

The dimensionless and discrete shape of this equation is as follows.

$$\frac{Power}{\rho g^{3/2}L^{7/2}}=\hat{P}_a=\frac{\hat{P}_k^2(t)}{\hat{K}_t} \quad (14)$$

The selected Lengths in the present question are chosen from Pico and Isle Islay models. To absorb more energy, the power plant is installed at a distance from the beach.

TABLE I
THE DETAILS OF THE INPUT WAVE AND GEOMETRIC DETAILS OF THE OWC POWER PLANT BASED ON FIG2

Amount	Dimensionless parameter	Definition	Amount	Parameter
0.0139	$\hat{A}$	Input wave domain	0.475	*A (m)*
2.517	$\hat{T}$	Incoming wave frequency period	4.7	*T (sec)*
0.439	$\hat{h}$	depth of water	15	*h (m)*
1	$\hat{L}$	Input wavelength	34.2	*L (m)*
0.537	$\Delta\hat{t}$	Time step	0.5	*Δt (sec)*
2.193	$\hat{X}_{front}$	Front distance	75	X_{front} *(m)*
0.585	$\hat{X}_{behind}$	The back wall of OWC to the shore	20	X_{behind} *(m)*
0.292	$\hat{X}_{fs}$	Free surface length inside the chamber	10	X_{fs} *(m)*
1.8625	$\hat{K}_t$	Turbine Drop Coefficient	119.4	K_t
75	θ	OWC wall angle against free surface	75	*θ (degree)*

B. 3D OWC with parabolic side walls

OWC with parabolic side walls was investigated in 3D numerical model. as shown in Fig. 4. The problem of this

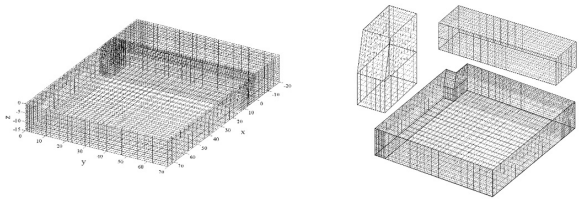

Fig. 3. Quadrilateral mesh on surfaces of three zones and quadrilateral mesh on whole of the solution domain.

study divided into two parts and one of these parts was solved due to symmetry. Fig. 4 shows the geometry of the problem.

The mathematical formula for parabolic shape is:

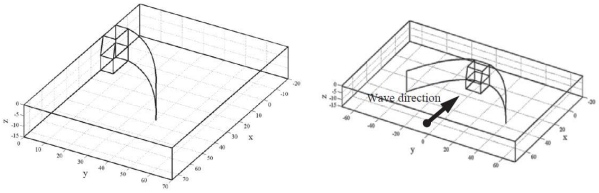

Fig. 4. Geometry of the OWC with parabolic side walls.

$$x=\frac{-2x_{facus}+\sqrt{4x_{facus}^2+b^2}}{b^2}y^2+\frac{2x_{facus}-\sqrt{4x_{facus}^2+b^2}}{4}, \quad (15)$$

Where x and y are coordinate axes according to Fig. 4, x focus is focus of the parabola and b is the width of OWC.

In this section 3D numerical modelling of OWC chamber with parabolic side walls was investigated. Quadrilateral meshes generated on boundaries of three zones. Fig. 5 shows mesh design on the geometry of solution domain and three zones close to each other.

For nearly singular points in BEM, analytical

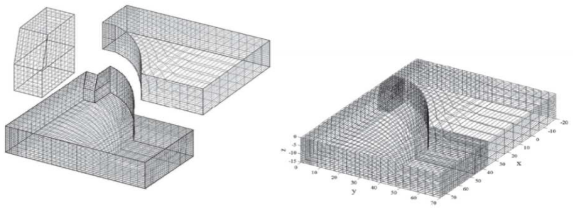

Fig. 5. Quadrilateral mesh on surfaces of three zones and quadrilateral mesh on whole of the solution domain.

integration was used instead of Gauss integration. This caused convergence in time marching [14]. The results of this study were compared with Josset and Clement research. Fig. 6 shows the comparison between present study and mentioned research for a specified OWC chamber. Also, capture width parameter $\varepsilon=\frac{P_{mt}}{P_{mi}}$ was compared with Josset and Clement results. In this formulation, P_{mt} is air power passing from turbine and P_{mi} is incident power per meter of wave crest.

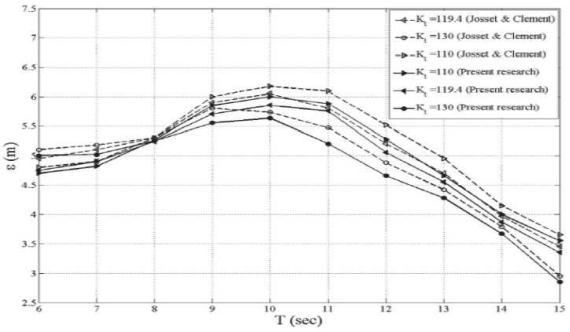

Fig. 6. Capture width of Pico Plant OWC versus wave period (wave amplitude=0.78m).

The overall shape of the diagrams in Fig. 6 is similar to each other but the calculated results in the present study is slightly lower than the results of the Josset and Clement research, This can be due to the slight difference in the geometry of the two power plants in the two studies. The amount of absorbed air power of OWC is shown in a comparison of two studies using the following equation in Fig. 7

$$P_{mi}=\frac{\rho g^2}{8\pi}A^2T` \quad (16)$$

In which incident wave period is T and incident wave amplitude is A.

The considered 3D BEM model was previously

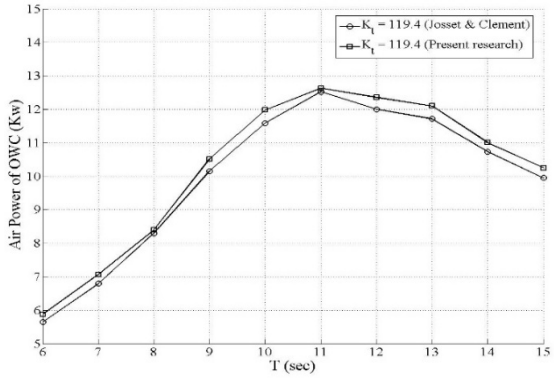

Fig. 7. The power of air passing through the turbine in different periods in kilowatts.

validated with Josset and Clement research. The results shown in Fig. 6 and 7 illustrate a good accordance between these two studies. For more information, refer to the article provided by the author [15].

In the chart below, the dimensionless Partial pressure of free surface diagram in two model of the OWC with flat side walls and with parabolic side walls) has been shown. This chart is in the range of almost one period. In the dimensionless time range of 13.39 to 16.34 solution was reached stable and oscillation of partial pressure of water free surface in the chamber alternatively iterate. This time range is equal to 25s-35s.

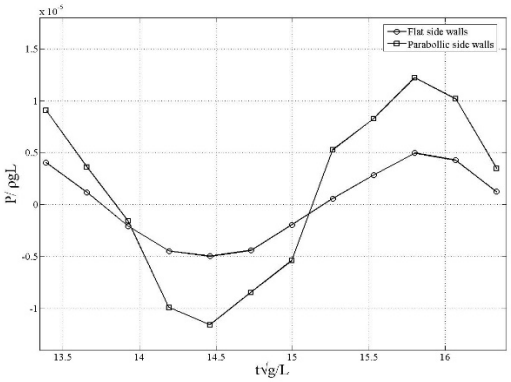

Fig. 8. The comparison dimensionless Partial pressure of water free surface inside the chamber of 2 model.

As we can see in the diagram, the maximum pressure of the OWC with parabolic side walls is 2.5 times as maximum pressure of the OWC with flat side walls. In is worth to mention that the average of the Partial pressure of water free surface in the OWC with the flat side walls is almost zero but this is more than zero in the OWC with parabolic side walls. This fact shows that oscillation of water inside the chamber transfer more energy to the turbine.

IV. 2D NUMERICAL MODEL OF OWC

In this section, performance of 3 types of OWC with different dimensions as a wave energy converter and breakwater was studied numerically. Finally, the best model was selected.

To create a free surface in the CFD programs, the domain must somehow be divided into two phases of a fluid. Fluent can model the effects of open-channel flow using a Volume of Fluid (VOF) formulation. Because of the amount of turbulence in this system the Shear Stress Transport (SST) k-omega turbulence model is implemented to the Reynolds Stresses in RANS equations. The materials and their properties used for this are fairly simple. Only two fluids were necessary for this project, water in liquid form, and air, their materials and properties can be seen from the table II.

TABLE II
THE MATERIALS PROPERTIES.

Air density	1.225	$\frac{Kg}{m^3}$
Air viscosity	$1.7894*10^{-5}$	$\frac{Kg}{m.s}$
Water density	998.2	$\frac{Kg}{m^3}$
Water viscosity	0.001003	$\frac{Kg}{m.s}$

In the 2D numerical wave tank, the top of the model (AC) opening of the tank was modelled as a pressure inlet boundary, with the pressure set to a gauge pressure of zero. The bottom (BD) was modelled as a no-slip wall. The inlet, (AB) or Flap type wave generator, was simple a velocity inlet that made use of the open cannel wave boundary function in Fluent. The boundary (CD) was modelled as pressure outlet that make use of open channel boundary function There is a danger with using this function because it involves some wave reflections which are higher than the fixed fluid surface. Therefore to reduce the unwanted reflected waves from outlet boundary, the numerical beach function is used in the model. This function allows for damping of incoming waves which was found to work effectively to eliminate the reflections completely.

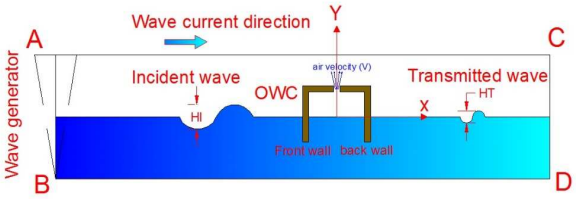

Fig. 9. The sketch of the OWC device and wave tank.

During the investigation wavelength (L) was constant (1.5 m). According to different incident wave heights(H_I) , 0.1, 0.14, 0.18, 0.22, models were examined. The Depth of water was 1.35 m during the numerical study.

In the first and the second model the length of the back and front wall of OWC was considered the same size but their levels from the water free surface were different, the third model is a combination of these 2 types of model.

Mesh designing is so important to get good results from the model. The quality of the conclusions depends on the mesh and time step size. Quadrilateral elements are used in the model. Due to improving the quality of the mesh design and reducing the time steps, mesh dimensions around the OWC are smaller than the other areas. Total cells are counted 6292 faces and nodes count 12799 and 6506 respectively. The sketch of these 3 types of model and mesh design can be seen in the fig. 10-11.

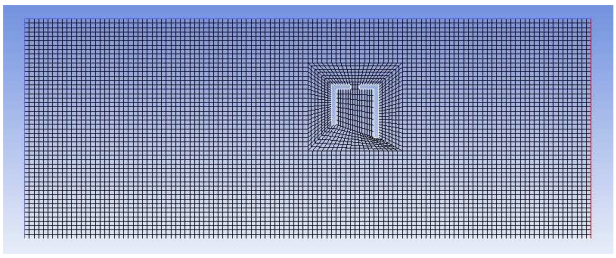

Fig. 10. Mesh design.

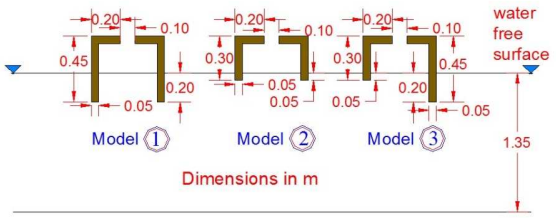

Fig. 11. The sketch of 3 types of models.

Fig. 12 shows snapshots of the water surface profile and different phases in the wave tank. In this figure, to create a free surface in the CFD program, the domain must somehow be divided into two phases of a fluid. Fluent can model the effects of open-channel flow using a Volume of Fraction (VOF) formulation, the water free surface configuration is defined as the VOF function, F = 0.5.The wave transformations around the OWC and the wave attenuation can be carefully investigated using fig. 12 and fig. 13 shows velocity vectors and its magnitude around the OWC.

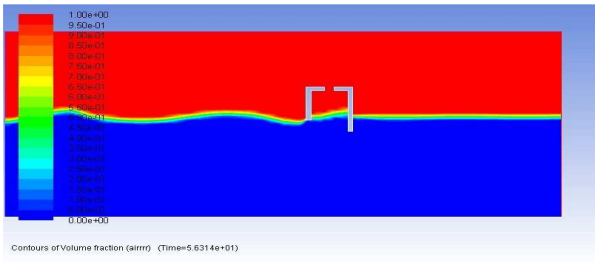

Fig. 12. Wave attenuation in numerical study.

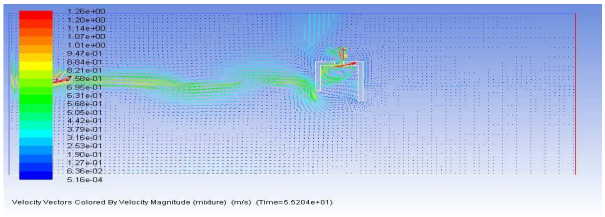

Fig. 13. Velocity vectors around floating OWC.

Wave attenuation is calculated by equation ($1-\frac{H_T}{H_I}$). In this equation the transmitted wave height is defined as (H_T) and the incident wave height is defined as(H_I). In the table I (V) is air velocity from the orifice and (L) is wave length.

TABLE III
RESULTS EXTRACTED FROM THE 2D NUMERICAL MODELS

Model	L(m)	H_I(m)	H_T(m)	Wave Attenuation	V(m/s)
1	1.5	0.1	0.007	0.93	0.27
1	1.5	0.14	0.008	0.94	0.3
1	1.5	0.18	0.01	0.94	0.32
1	1.5	0.22	0.012	0.94	0.33
2	1.5	0.1	0.055	0.45	0.91
2	1.5	0.14	0.058	0.58	1.05
2	1.5	0.18	0.06	0.66	1.20
2	1.5	0.22	0.062	0.71	1.46
3	1.5	0.1	0.01	0.9	0.92
3	1.5	0.14	0.016	0.88	1.17
3	1.5	0.18	0.018	0.9	1.25
3	1.5	0.22	0.02	0.9	1.34

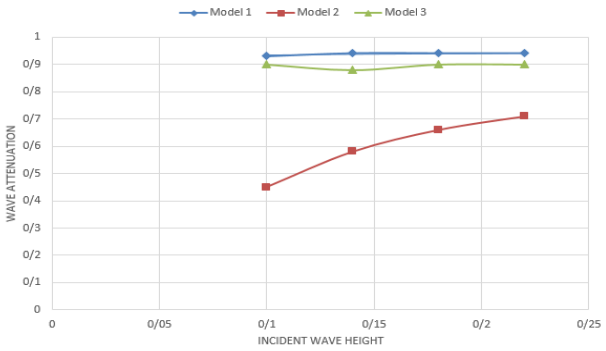

Fig. 14. The numerical simulation results of wave attenuation (Wave length 1.5 m).

During the numerical tests it has been observed that the water free surface inside the chamber oscillating like an oblique slanting line so if a buoyant moving surface which is free to move up and down like a piston is used inside the chamber it could move more volume of trapped air inside the chamber so more energy can be produced.

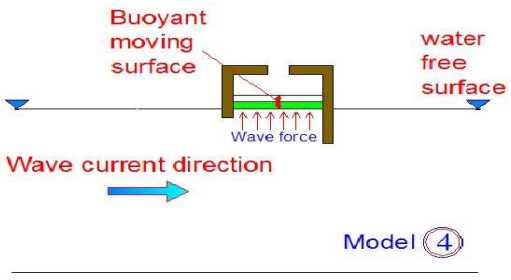

Fig. 15. Floating OWC with buoyant moving surface.

V. CONCLUSION

The performance of offshore stationary OWC device as a wave energy convertor and a floating breakwater have been numerically investigated. In order to do that, 2 types of OWC models compered numerically, Three-dimensional OWC with parabolic side walls and OWC with flat side walls. According to the results of 3D numerical models, the maximum air pressure of the OWC with parabolic side walls is 2.5 times as maximum air pressure of the OWC with flat side walls, so OWC with parabolic side walls shows better performance compared to the other one and oscillation of water inside the chamber transfer more energy to the turbine.

In the second part of investigation, 3 types of OWC device with different dimensions have been modelled and impacts of increasing the incoming wave height was analyzed.

After some tests by a comparison between model 1 and 2, it was obvious that model 1 reflected wave energy more than model 2 and it attenuated about 90 percent of incident wave height, but less energy can be extracted by model 1 compared to model 2 and 3.

Model 2 allows the waves pass the OWC but it extracts more wave energy compered to model 1 and the water surface level inside of the OWC fluctuated more than model 1.

Finally, model 3 cover the deficiency of both models, in this model the amount of wave attenuation was in good rang. Because the length of front wall is shorter than the back wall, it lets wave enter the chamber and back wall does not allows it pass the OWC so the water surface level fluctuates more in the chamber and it increases the trapped air inside the chamber so the air pressure, increases power generation by turbines. Therefore, as the length of the back wall of the OWC increases, more energy is absorbed so model 3 shows the better performance compared to the two other models.

Finally, because of the rise and fall of inner free-surface oscillating like an oblique slanting line, using a buoyant moving surface which is free to move up and down inside the chamber can increase the performance of the OWC device.

This study shows OWC devices absorb wave energy and convert to other form of energy also they can be used as a floating breakwaters therefore using OWC devices are more Cost-effective compare to other form of wave energy converters and breakwaters.

REFERENCES

[1] D. V. Evans. "Oscillating water column wave energy convertors," *J. IMA Journal of Applied Mathematics*., vol. 22, pp. 423–433, 1978.

[2] D. V. Evans. "Wave power absorption by systems of oscillating surface pressure distributions," *J. Journal of Fluid Mechanics.* , vol. 114, pp. 481–499, 1982.

[3]. K.Thiruvenkatasamy, S.Neelamani and M.Sato. "Nonbreaking wave forces on multiresonant oscillating water column wave power caisson breakwater," *J. Journal of Waterway, Port, Coastal and Ocean engineering.* , vol. 131, no. 2, pp. 77-84, 2005.

[4]. C.Josset and A.H.Clement, "A time-domain numerical simulator for oscillating water column wave power plants," *Renewable Energy*. vol. 32, no. 8, pp. 1379–1402, 2007.

[5] J. Henriques, A. Falcao, R. Gomes, L. Gato, "L.M.C. Latching Control of an Oscillating Water Column Spar-Buoy Wave Energy Converter in Regular Waves," *J. Journal of Offshore Mechanics and Arctic Engineering*. vol. 135 no. 2, 2013.

[6] A. McKinley, P. Lamont-Kane, A. Henry, M. Folley, J. Nicholson, T. Whittaker, B. Elsaesser, "Preliminary development of a Pseudo-3D testing technique for the prediction of extreme loads on an oscillating wave surge converter," *3rd Asian wave and tidal energy conference*, Singapore, vol. 2 , 2016.

[7] A. Elhanafi, "Prediction of regular wave load on a fixed offshore oscillating water column-wave energy converter using CFD," *J. Journal of Ocean Engineering and Science*, vol. 1, no. 4, pp. 268-283, 2016.

[8] A. Elhanafi, G. Macfarlane, A. Fleming, Z. Leong, "Experimental and numerical measurements of wave forces on a 3D offshore stationary OWC wave energy converter," *J. Journal of Ocean Engineering,* vol. 144, pp. 98-117, 2017.

[9] P. Lubin, S. Vincent, S. Abadie, J. Caltagirone, "Three-dimensional Large Eddy Simulation of air entrainment under plunging breaking waves," *J. Coastal Engineering*. Vol. 53, no. 8, pp. 631-655. 2006.

[10] Wilcox. D. C, "Turbulence Modeling for CFD," California, USA: DCW Industries, Inc., La Canada, California. 1993.

[11] Menter. F. R. "Two-Equation Eddy-Viscosity Turbulence Models for Engineering Applications," *J.AIAA Journal,* vol. 32(8), pp. 1598–1605. 1994.

[12] R.G. Dean, R.A. Dalrymple, "Water wave mechanics for engineers and scientists," World Scientific, 3rd edition, USA, 1991.

[13] E.Zauderer, "Partial differential equations of applied mathematics," Wiley (Interscience), third edition, 2011.

[14] M. Abbaspour, M.H. Ghodsi, "Design of a new scheme to indicate the domain of applicability of near singular approach in 2D BEM," *Engineering Analysis with Boundary Elements*, vol. 35, no. 1, pp. 129-139, 2011.

[15] M. H. Ghodsi, "Free surface modeling in OWC chamber with parabolic side walls using 3D BEM," *AIP Conference Proceedings*, 1648, 2015.